Supplementary Materials for

Templated growth of vertically aligned 2D metal-organic framework nanosheets

Hui Li, [1] Jingwei Hou, [2*], Thomas D. Bennett[2], Jindun Liu, [1] Yatao Zhang [1**]
[1] School of Chemical Engineering and Energy, Zhengzhou University, Zhengzhou 450001, P. R. China
[2] Department of Materials Science and Metallurgy, University of Cambridge, CB3 0FS, Cambridge, UK

* Corresponding authors: E-mail address: jh2131@cam.ac.uk; zhangyatao@zzu.edu.cn

This PDF file includes:

Figures S1 to S14
Tables S1
References

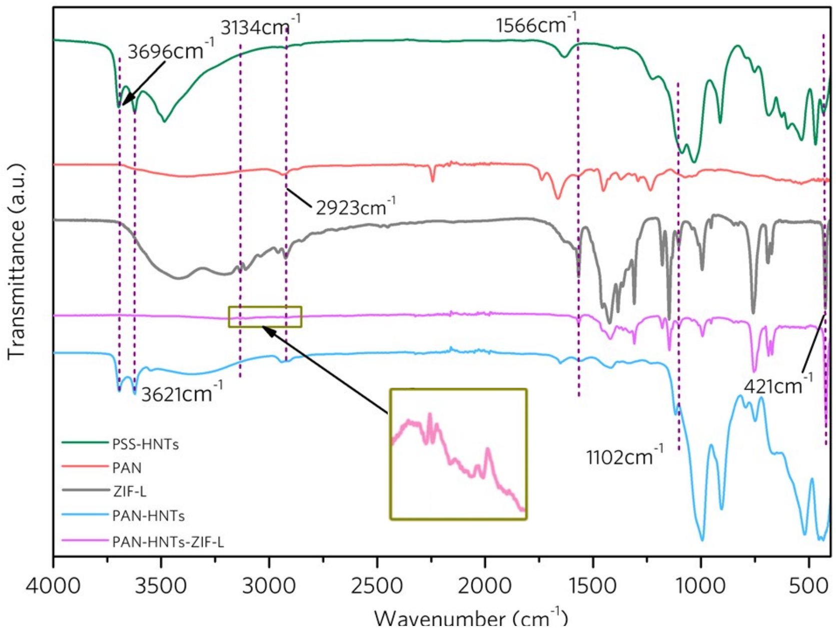

Figure S1 ATR-FTIR spectra of the ZIF-L crystal, PSS-HNTs powder and the membrane with different treatment.

To fabricate a continuous and coherent ZIF-L layer, the PAN membrane was firstly modified with halloysite nanotubes (HNTs). The change of membrane surface chemical properties was characterized by FT-IR and the resulted spectra are presented in Supplementary Figure S1. The IR spectrum of the PSS modified HNTs was in well agreement with the spectrum reported previously. The characteristic peaks at 3696 and 3621cm^{-1} belonged to the stretching vibration of hydroxyl groups of HNTs, and a strong adsorption at 1000 cm^{-1} originated from the asymmetric flexible vibration of O–Si bond due to the plenty of O–Si–O groups on the outer surface of HNTs. The peak at 1229 cm^{-1} and 1102 cm^{-1} were ascribed to the characteristic peaks of sulfonate groups.

The PAN substrate had characteristic peaks at 2922 and 2862 cm^{-1} which were ascribed to the stretching vibration of -CH_2- or -CH_3 of the backbone, and a peak at 2243 cm^{-1} corresponded to the stretching vibration of -C≡N. After coating with PSS-HNTs layer on the PAN substrate, main characteristic peaks of PSS-HNTs at 3696 and 3621 cm^{-1} emerged.

The IR spectrum of the pure ZIF-L crystals included C-H stretching within the methyl (C-CH_3) groups and aromatic at around 3134 cm^{-1} and 2923 cm^{-1}, the C=N stretch of the imidazole ring (1580 cm^{-1}), Zn-N at 421 cm^{-1}, and the convoluted bands at 500-1500 cm^{-1} were related to the imidazole ring stretching, ring in-plane bending and ring out-of-plane bending. These signature bands were also identified on PSS-HNTs-ZIF-L membrane, indicating the presence of ZIF-L crystals on the top of membrane.

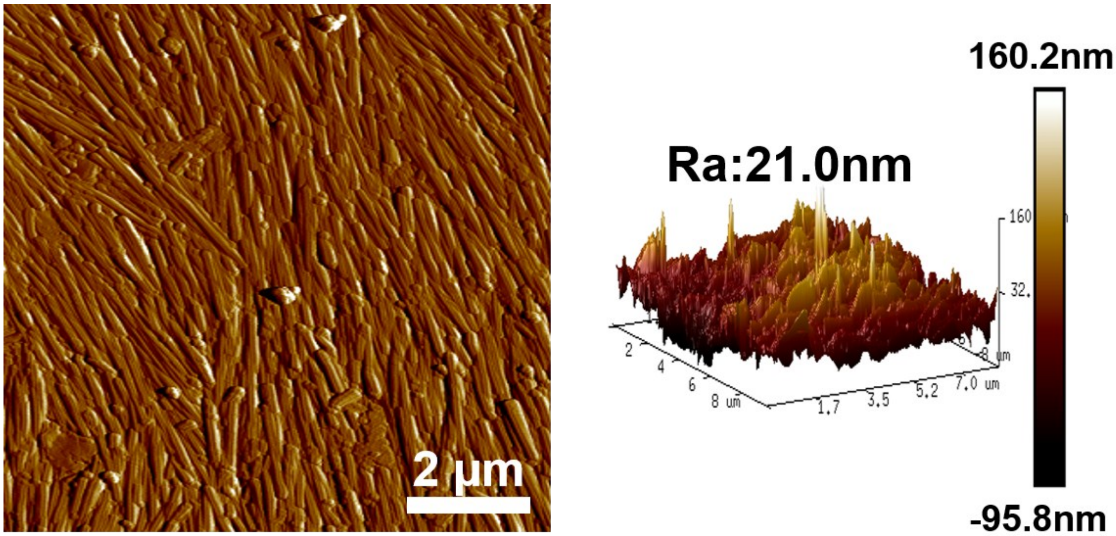

Figure S2 AFM images of PSS-HNTs coated membrane surface.

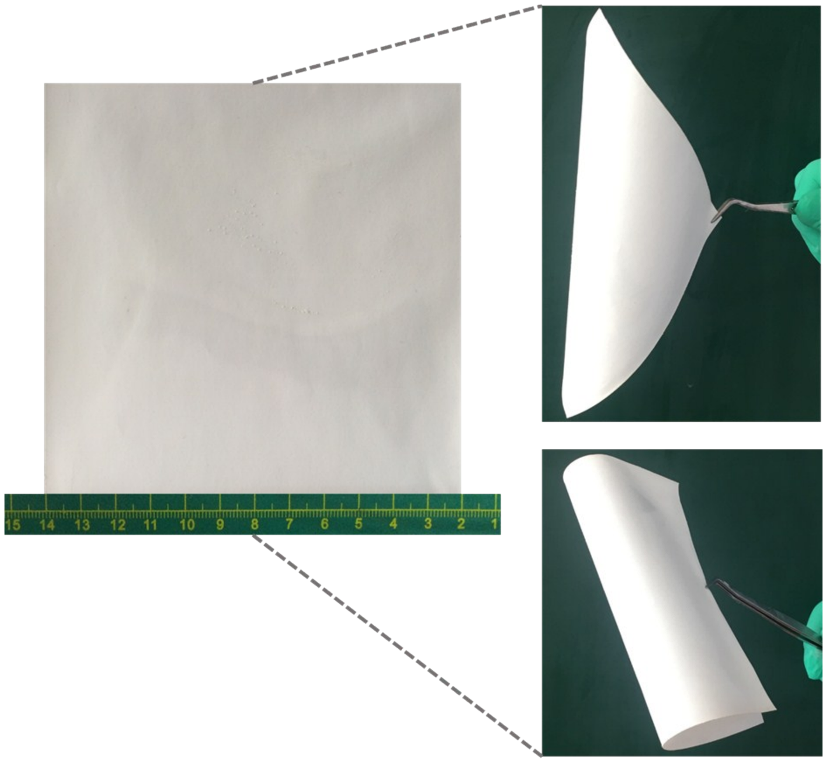

Figure S3 Optical image of the polymeric membrane supported ZIF-L (large size).

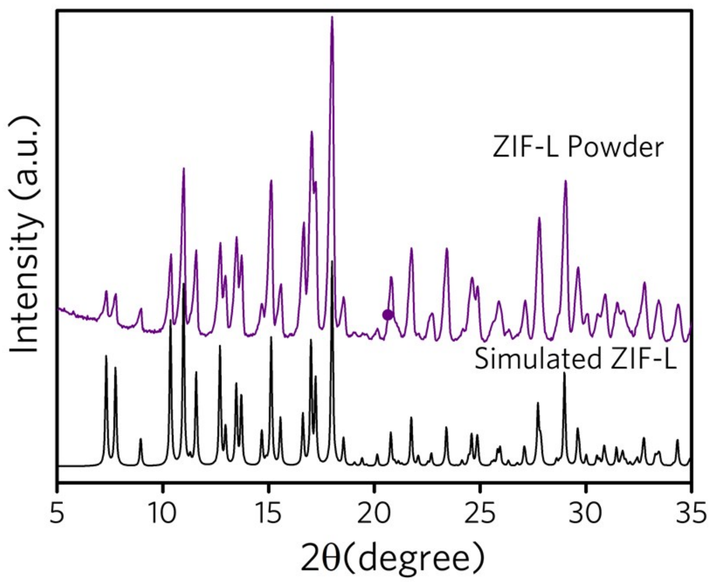

Figure S4 PXRD results for the synthesized ZIF-L powder and the simulated ZIF-L.

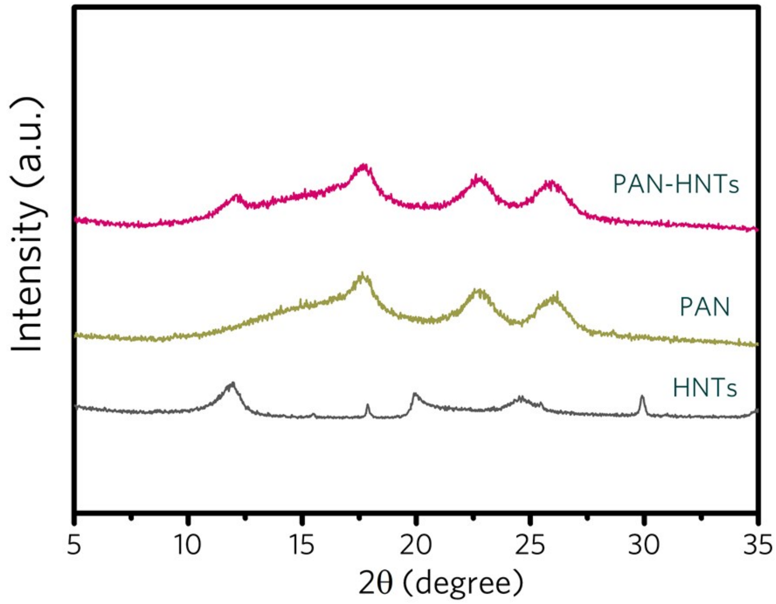

Figure S5 PXRD results for HNTs, PAN supporting membranes and HNTs coated PAN membranes.

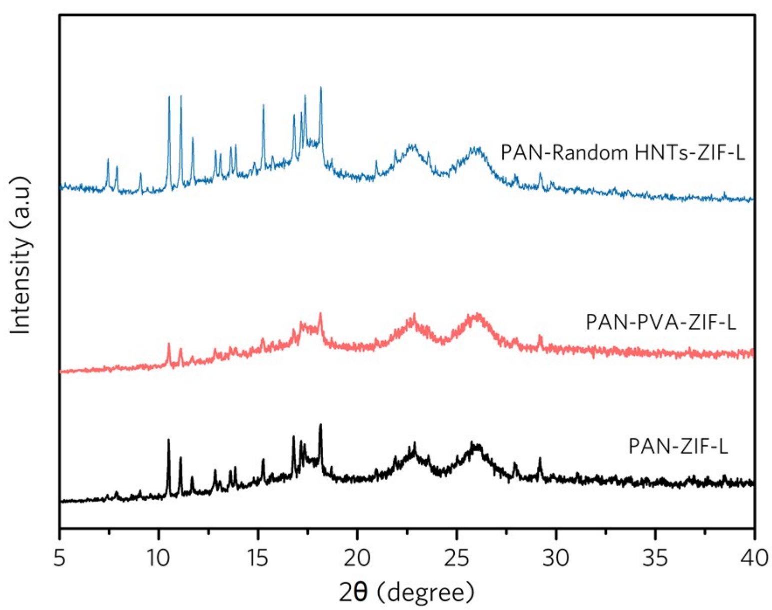

Figure S6 PXRD results for ZIF-L deposited on PAN polymeric membrane (PAN-ZIF-L), PVA modified PAN polymeric membrane (PAN-PVA-ZIF-L) and PAN membrane with randomly oriented HNTs coating (PAN-Random HNTs-ZIF-L).

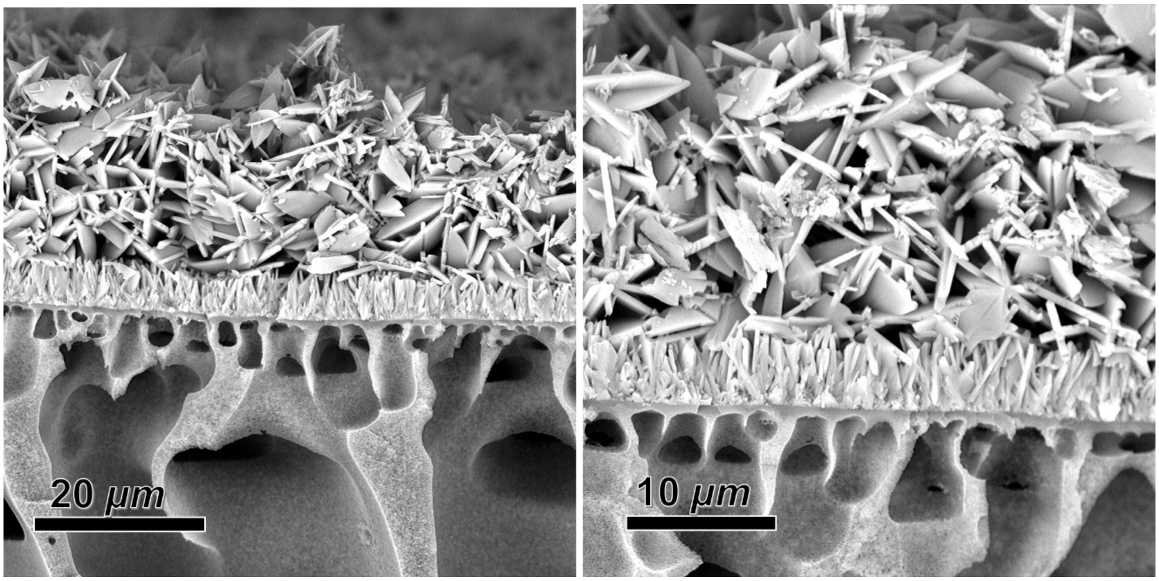

Figure S7 Direct ZIF-L deposition on un-modified PAN membrane surface.

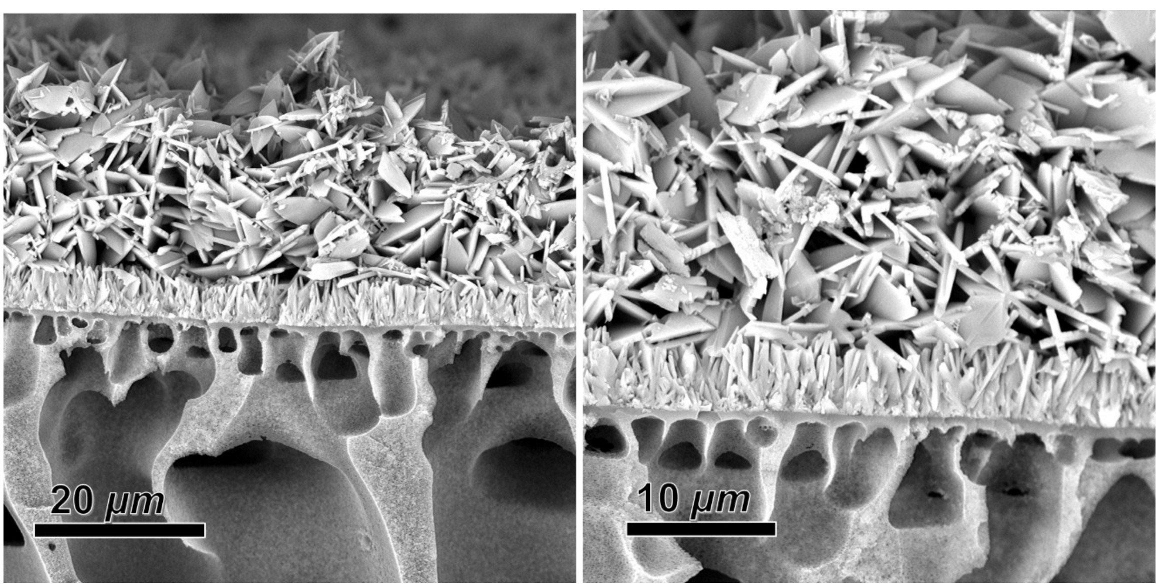

Figure S8 ZIF-L deposition on PVA modified PAN membrane surface.

For the PVA modification, the supporting PAN membrane was mounted in a membrane cell (effective area of 28.3 cm^2), followed by adding 3 mL of 0.06 wt % PVA solution and was dried in an oven at 80^oC.

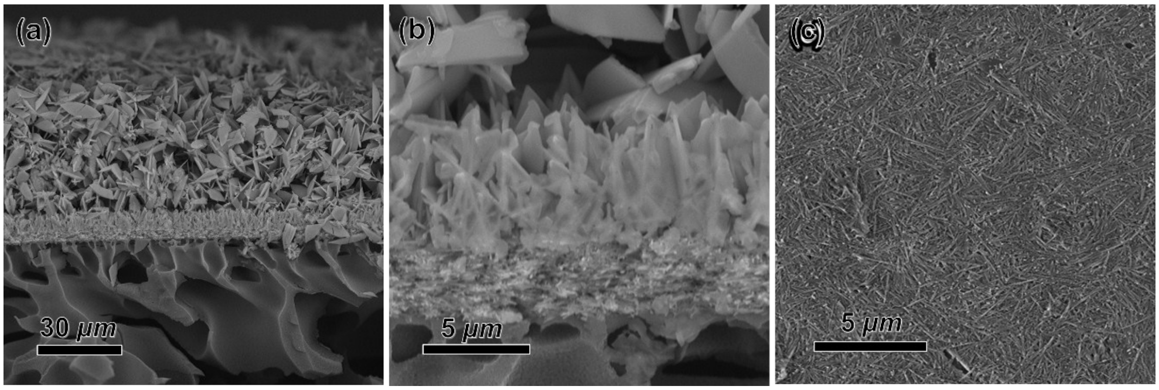

Figure S9 (a-b) ZIF-L growth on the randomly oriented HNTs coated membrane, and (c) surface morphology of the randomly oriented HNTs layer (without ZIF-L deposition).

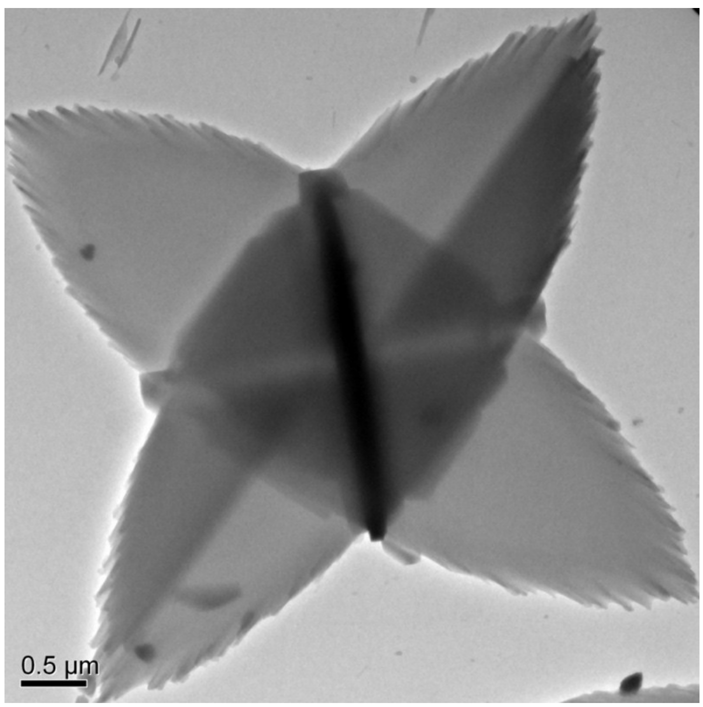

Figure S10 TEM image of the cross-leaf ZIF-L in suspension solution.

(a)

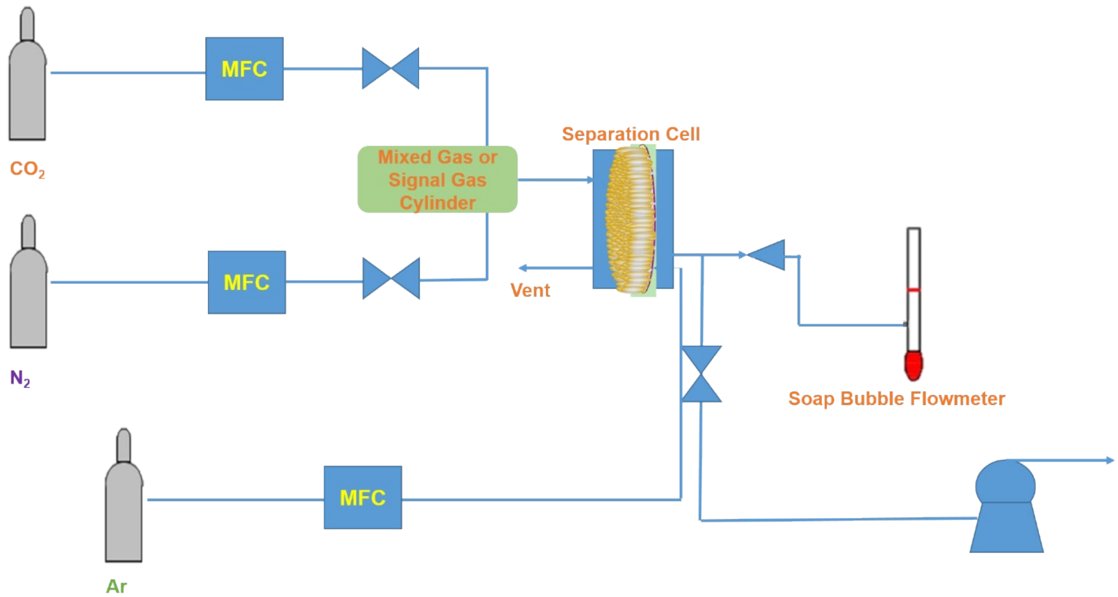

(b)

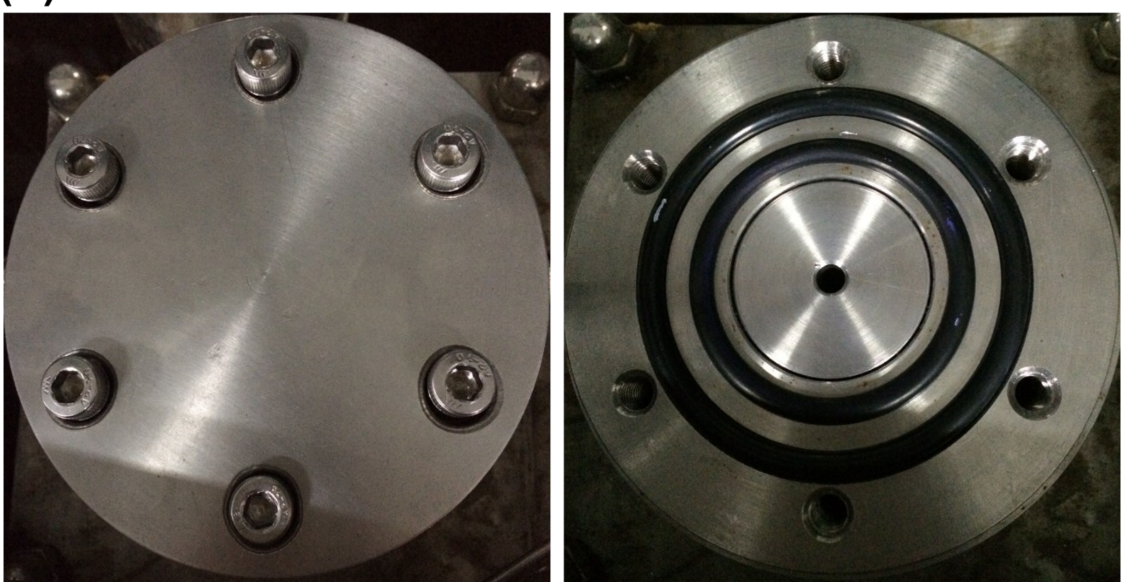

Figure S11 (a) Schematic diagram of a gas permeation set-up (Wicke-Kallenbach technique) and (b) photo of testing membrane module (effective membrane area of 19.6 cm^2).

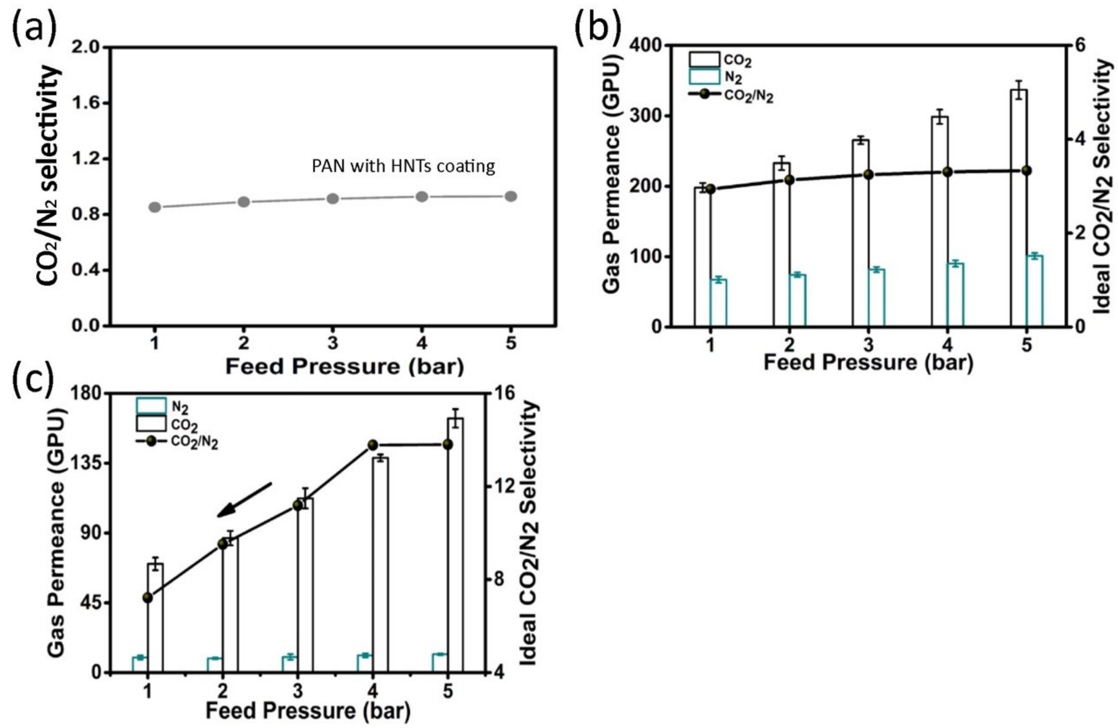

Figure S12 Gas separation performance for (a) PAN supporting membranes with PSS-HNTs coating, (b) membrane with ZIF-L deposited on randomly oriented HNTs; and (c) vertically ZIF-L membrane (with 8 h ZIF-L secondary deposition) performance during the depressurization process.

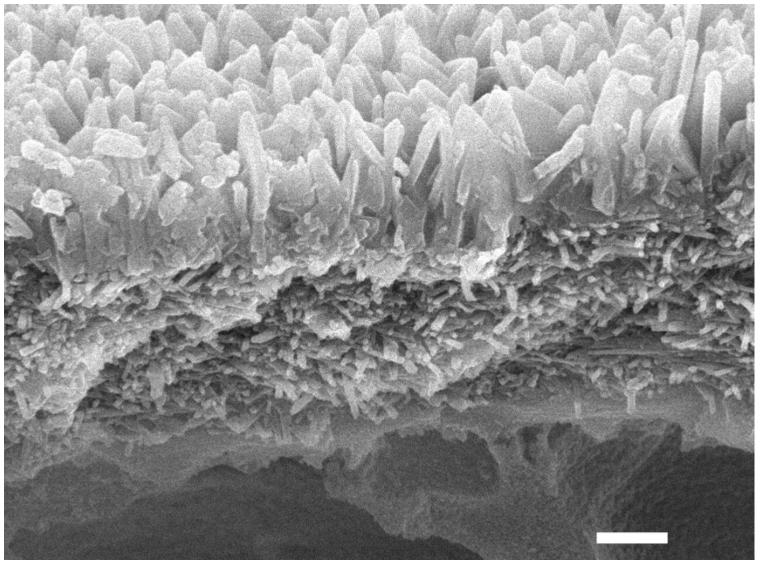

Figure S13 SEM image of the membrane cross-section with 4 hour secondary ZIF-L deposition. The scale bar is 1 μm.

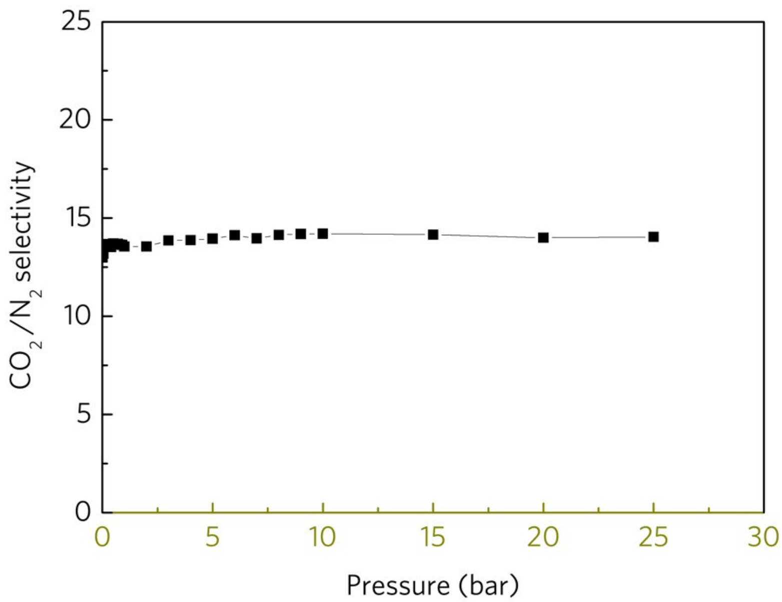

Figure S14 CO_2/N_2 gas adsorption selectivity based on molecular dynamic simulation.

Table S1 Comparison of single gas separation performance and ideal selectivities (CO_2/N_2) of the MOF membrane on various supports (Permeance 10^{-7}mol m^{-2} s^{-1} Pa^{-1})

Support		MOF materials	N_2 permeance	CO_2 permeance	Selectivity CO_2/N_2	References
Organic	PVDF hollow fiber	ZIF-8	25.77	28.56	1.11	Angew. Chem. (2016) [1]
	PVDF hollow fiber	ZIF-8	1.71	2.01	1.18	Chemistry-A European Journal (2015) [2]
		Cu-BTC	14.41	11.59	0.80	
	PAN hollow fiber	ZIF-8	-------	0.45	--------	J. Mater. Chem. A (2014) [3]
		Cu-BTC	188.82	171.96	0.91	
	BPPO hollow fiber	ZIF-8	2.11	1.60	0.76	Chemical Communications (2015) [4]
	Nylon hollow fiber	ZIF-8	34.10	--------	---------	Chemical Communications (2011) [5]
Inorganic	Alumina disk (flat sheet)	ZIF-8	15.94	20.5	1.29	Chemical Communications (2016) [6]
	Alumina disk (flat sheet)	ZIF-8	0.10	0.28	0.39	Chemical Communications (2016) [7]
	Alumina tube	ZIF-8	37.21	33.61	0.90	Chemical Communications (2012) [8]

References and Notes

1. J. Hou, P. D. Sutrisna, Y. Zhang, V. Chen, Formation of Ultrathin, Continuous Metal–Organic Framework Membranes on Flexible Polymer Substrates. *Angewandte Chemie International Edition* **55**, 3947-3951 (2016).
2. W. Li, Q. Meng, C. Zhang, G. Zhang, Metal-Organic Framework/PVDF Composite Membranes with High H_2 Permselectivity Synthesized by Ammoniation. *Chemistry - A European Journal* **21**, 7224–7230 (2015).
3. W. Li *et al.*, Stiff metal-organic framework-polyacrylonitrile hollow fiber composite membranes with high gas permeability. *Journal of Materials Chemistry A* **2**, 2110-2118 (2014).
4. E. Shamsaei *et al.*, Rapid synthesis of ultrathin, defect-free ZIF-8 membranes via chemical vapour modification of a polymeric support. *Chemical Communications* **51**, 11474-11477 (2015).
5. J. Yao *et al.*, Contra-diffusion synthesis of ZIF-8 films on a polymer substrate. *Chemical Communications* **47**, 2559-2561 (2011).
6. E. Shamsaei, X. Lin, L. Wan, Y. Tong, H. Wang, A one-dimensional material as a nano-scaffold and a pseudo-seed for facilitated growth of ultrathin, mechanically reinforced molecular sieving membranes. *Chemical Communications* **52**, 13764-13767 (2016).
7. X. Wang *et al.*, Improving the hydrogen selectivity of graphene oxide membranes by reducing non-selective pores with intergrown ZIF-8 crystals. *Chemical Communications* **52**, 8087-8090 (2016).
8. Z. Xie *et al.*, Deposition of chemically modified α-Al_2O_3 particles for high performance ZIF-8 membrane on a macroporous tube. *Chemical Communications* **48**, 5977-5979 (2012).